EURASIAN PHYSICAL TECHNICAL JOURNAL

2026, Volume 23, No. 1 (55)

https://doi.org/10.31489/2026N1/24-33

Received: 17/11/2025 Revised: 24/02/2026 Accepted: 19/03/2026 Published online: 30/03/2026

Research Article

UDC 539.232; 538.915; 535.215.6; 536.4; 620.91

PHOTOVOLTAIC PROPERTIES OF SILICON HETEROJUNCTION SOLAR CELLS FABRICATED ON BORON-DOPED SILICON WAFERS UNDER EXTRATERRESTRIAL ILLUMINATION

Utamuradova Sh.B.[1], Terukov E.I.[2], Ataboev O.K.[1*], Kabulov R.R.[3], Panaiotti I.E.[2], Uzakbayeva N.S.[4]

[1] Semiconductor Physics and Microelectronics Research Institute, Tashkent, Uzbekistan
[2] Ioffe Institute, Russian Academy of Sciences, St. Petersburg, Russia
[3] Physical-technical Institute Uzbekistan Academy of Sciences, Tashkent, Uzbekistan
[4] Nukus state technical university, Nukus, Uzbekistan

*Corresponding author: omonboy12@mail.ru

Abstract. *The temperature coefficient is a key performance indicator for assessing the operational stability of solar cells used for power generation in both terrestrial and space environments. In recent years, silicon heterojunction solar cells employing hydrogenated amorphous silicon passivating layers have attracted significant attention owing to their high conversion efficiency and excellent surface passivation quality achieved at low processing temperatures. However, to ensure their reliable and stable operation in extraterrestrial conditions, it is essential to investigate not only the effects of radiation but also the influence of temperature variations on their photovoltaic performance. In this study, the illuminated current–voltage characteristics of heterojunction solar cells fabricated on boron-doped single-crystalline silicon wafers were experimentally investigated under Air Mass Zero spectrum across a wide temperature range of 173–373 K. The results revealed that the short-circuit current density exhibited a positive temperature coefficient of +(0.077±0.003) %/K, whereas the open-circuit voltage decreased linearly with a coefficient of – (0.23±0.002) %/K as temperature increased. The temperature coefficients of the conversion efficiency and fill factor were determined to be – (0.23±0.007) %/K and – (0.075±0.004) %/K, respectively. The experimentally obtained temperature coefficient of the maximum output power – (0.231±0.008) %/K was found to be lower than that of conventional Al-BSF solar cells (−0.39%/K) and other single-crystalline silicon–based photovoltaic technologies, confirming the excellent thermal stability and high suitability of silicon heterojunction solar cells for space power applications.*

Keywords: heterojunction, hydrogenated amorphous silicon, Air Mass Zero spectrum, light current-voltage characteristics, temperature coefficient, open-circuit voltage, conversion efficiency.

1. Introduction

It is well known that reliable broadband Internet access and data transmission, particularly in remote regions where stable communication networks are lacking, can be achieved through the deployment of global low Earth orbit (LEO, 500–2000 km altitude) satellite communication systems [1-3]. The continuous and efficient operation of such satellites depends on the availability of highly reliable power supply systems. In these spacecraft, electrical energy is primarily generated by photovoltaic (PV) modules [4, 5]. Therefore, enhancing the efficiency, radiation resistance, and thermal stability of PV modules is essential to ensure the long-term and stable operation of satellite communication systems in LEO [6].

Since the launch of the first Soviet satellite, *Sputnik 1*, in 1957, interest in solar cells (SCs) has increased significantly [4]. One year later, in 1958, Si-based SCs were used for the first time aboard the *Vanguard-1* satellite launched by the United States [7]. Since then, Si SCs have been widely adopted as the primary power source for spacecraft because of their long-term operational stability, mature fabrication technology, and favorable power-to-mass ratio [4, 8, 9]. This trend continued until the 1990s, when the development of Si-based SCs for space applications was largely discontinued, and research efforts shifted toward III–V compound semiconductor-based SCs, which subsequently began to dominate the space market [5, 7]. At present, the most widely used semiconductor materials for space applications - particularly in geostationary Earth orbit (GEO, at an altitude of approximately 35.786 km above Earth's surface) - are GaAs-based multijunction SCs, such as GaInP/GaInAs/Ge [5] and AlInGaP/AlInGaAs/InGaAs/Ge [10]. However, the production cost of these SCs is considerably higher than that of their Si-based counterparts, primarily due to the complex technological processes required for their fabrication [5, 11]. In addition, the brittle nature of GaAs compounds further complicates large-scale manufacturing and handling. These factors have limited the widespread adoption of GaAs-based SCs for terrestrial applications and, in particular, for use in LEO missions, where cost efficiency and structural robustness are of critical importance [4].

Currently, among Si-based PV technologies, Si heterojunction (HJT) SCs have emerged as the most efficient option. A record conversion efficiency of 27.8% has been achieved for n-type heterojunction back-contact (HBC) SCs with an active area of 134 cm², developed by LONGi Laboratory under standard test conditions (1 sun, AM1.5G, 100 mW/cm²) [12]. This represents the highest efficiency reported for any single-junction Si-based SC and is comparable to that of state-of-the-art single-junction GaAs SCs (29.1%) [12, 13]. Moreover, HJT SCs exhibit a higher bifacial coefficient compared with other Si-based PV technologies [13]. Owing to the use of low-temperature hydrogenated amorphous silicon (*a*-Si:H) passivating layers and low Si consumption, HJT SCs achieve exceptionally high open-circuit voltages (up to 752 mV) and low temperature coefficients (< 0.3%/°C for n-type wafers). These characteristics provide a significant advantage over other Si-based PV technologies such as PERC (Passivated Emitter and Rear Cell), TOPCon (Tunnel Oxide Passivated Contact), and conventional Al-BSF (Aluminum Back Surface Field), which currently dominate terrestrial PV manufacturing [14-16]. In contrast, these alternative technologies generally require high-temperature processing (> 600 °C) [15]. The combination of superior efficiency, low-temperature fabrication, and outstanding thermal stability makes HJT SCs highly promising candidates for space PV applications. In extraterrestrial environments - particularly in LEO, the performance of SCs is affected not only by high-energy particle irradiation but also by extreme cyclic temperature fluctuations (160–400 K) [8, 17]. Therefore, a comprehensive study of the temperature-dependent behavior of HJT SCs under extraterrestrial solar illumination is essential for evaluating their reliability and long-term operational stability in future spacecraft power systems.

In this study, the temperature dependence of the PV performances of HJT SCs based on boron-doped p-type crystalline Si (c-Si) wafers were investigated under Air Mass Zero (AM0) spectrum (136.7 mW/cm²) in the temperature range of 173–373 K.

2. Material preparation and methods

2.1 Sample preparation

The studied p-type Si HJT SCs were fabricated at the R&D Center of Thin film technologies in Energetics, Saint-Petersburg, Russia. To conduct experiments, Si HJT SCs (Fig. 1) were created on boron-doped p-type c-Si wafers grown by the Czochralski method, with an acceptor concentration of $3 \cdot 10^{16}$ cm^{-3}, a thickness of ~165 μm, crystallographic orientation (100). In the c-Si wafer, the concentrations of oxygen and carbon, as well as density of dislocation were approximately $4.5 \cdot 10^{17}$ cm^{-3}, $3 \cdot 10^{16}$ cm^{-3} and 500 cm^{-2}, respectively. The wafers were acquired from SAS Sunrise and are commonly used in the fabrication of PERC SCs. Before depositing intrinsic and doped *a*-Si:H layers onto the p-type c-Si wafers to form the heterojunctions, the wafers underwent a wet chemical cleaning procedure. Afterward, the c-Si wafers were subjected to pyramidal surface texturing to enhance light absorption [18]. Subsequently, thin intrinsic *a*-Si:H layers were deposited on both the front and rear surfaces of the textured p-type c-Si wafers using Very High Frequency Plasma-Enhanced Chemical Vapor Deposition (VHF PECVD) method. The purpose of this layer is to passivate dangling bonds (by forming Si–H bonds**)** on the c-Si surfaces [19]. Using the same method to form a p-n-junction, n-type *a*-Si:H layer was deposited on the front side, and to create the back-surface field

(BSF), *p*-type *a*-Si:H layer was deposited on the rear side of *i*-*a*-Si:H deposited *p*-type c-Si wafer. All intrinsic and doped *a*-Si:H layers were deposited at a low temperature of 180–185°C and a frequency of 40.68 MHz. Further, transparent and conductive Sn-doped In_2O_3 (ITO) layers (90 wt.% In_2O_3 and 10 wt.% SnO_2) were deposited on the front and rear surfaces of the photosensitive heterostructures using Radio-Frequency (RF) magnetron sputtering. To collect photogenerated charge carriers from the heterostructure surfaces, low-temperature silver (Ag) paste with "Busbar" type contacts was screen-printed onto both the front and rear sides of the photosensitive heterostructures with subsequent curing. The "Busbar" type contacts had the following dimensions, measured using a KLA/Tencor Alpha-Step D-120 profilometer: a height of ~25 μm, a width of ~45 μm, and a pitch of ~1.36 mm**.** A cross-sectional view of the finished HJT SCs based on *p*-type c-Si wafer is shown in Fig. 1.

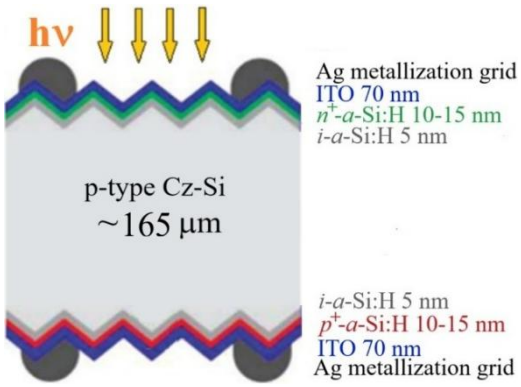

Fig. 1. A cross-sectional view of the HJT SCs based on *p*-type c-Si wafer.

2.2 Characterization and measurement of performances

As reported in [20, 21], in order to improve the overall efficiency of PV modules compared with conventional full-cell designs, standard SCs are divided into half-cells, which reduces the cell current and minimize resistive losses. This design also prevents the performance degradation of PV modules under partial shading conditions, which would otherwise increase resistance and potentially lead to module failure [21]. Therefore, two main techniques are currently employed for SC separation: laser scribing with mechanical cleaving (LSMC) and thermal laser separation (TLS) [20]. In the present study, *p*-type c-Si-based samples with an area of 1 × 1 cm^2 were cut from full-sized high-efficiency HJT SCs (15.6 × 15.6 cm^2) using the LSMC method for experimental investigation. No additional passivation of the lateral surfaces or edge isolation was performed after laser cutting. A solid-state "MiniMaker2" diode laser, with a wavelength of 1064 nm was used for cutting the samples. During laser scribing, the laser parameters were set as follows: a scribing speed of 200 mm/s, a pulse repetition rate of 25 kHz, and a pulse duration of 20 ns. The scribing process was carried out on the rear side of the *p*-*n*-junction, which helped to reduce potential damage to the contact layers and maintain photoelectric conversion efficiency.

To study the effect of temperature on the PV performance of *p*-type c-Si HJT SCs, light J-V curves were measured using a liquid nitrogen cryostat (Janis VPF-100). During the measurements, the samples were illuminated with a class AAA pulsed solar simulator (SS-80AAA simulator) under AM0 spectrum (136.7 mW/cm^2). The short-circuit current density and open-circuit voltage were recorded using a Keithley SM2460 Source Meter. Temperature stabilization during the measurements was maintained by the liquid nitrogen cryostat, equipped with a Lake Shore Model 335 temperature controller. Each light J-V measurement was conducted after the target temperature was reached and maintained for 4-5 minutes under the AM0 spectrum. Temperature coefficients of the output parameters of the HJT SCs, such as open-circuit voltage (V_{oc}), short-circuit current density (J_{sc}), fill factor (FF), maximum power (P_{max}) and conversion efficiency **(η)** were extracted from the slopes of the linear regions of the experimental temperature-dependent curves. For the present investigation, about 20 HJT SCs were fabricated. These samples exhibited similar parameters within a margin of error of no more than 2%. Among them, three representative samples were selected for temperature-dependent measurements, and their results are presented in this study.

This study focuses on characterizing the temperature-dependent performance of p-type c-Si HJT SCs without considering radiation effects.

3. Results and discussion

To investigate the influence of temperature on the PV parameters of the illuminated J-V curves of HJT SCs based on p-type c-Si, measurements were carried out under AM0 spectrum (136.7 mW/cm²) in the temperature range of 173–373 K (Fig. 2). As shown in Fig. 2, temperature has a significant effect on the shape of the illuminated J-V curves. In particular, the J_{sc} increases slightly with rising temperature, whereas the V_{oc} exhibits a pronounced decrease. It can also be seen from Fig. 2 that, at elevated temperatures, the influence of the series resistance (R_s) on the J-V curve shape becomes less pronounced, as a noticeable increase in J_{sc} is observed in this range. To determine the temperature dependence of each PV parameter of the p-type HJT SCs, namely the $V_{oc}, J_{sc}, FF, P_{max}$ and η, their variations with temperature were analyzed.

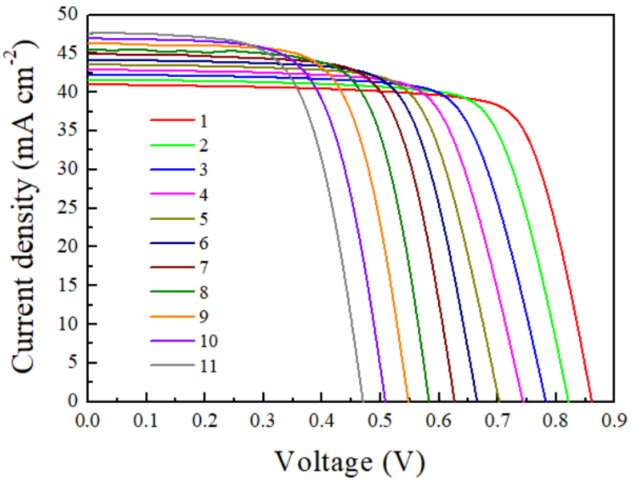

Fig. 2. Light J-V curves of HJT SCs based on p-type c-Si wafer under AM0 spectrum (136.7 mW/cm^2) in the temperature range of 173–373 K. T, K: 1 – 173, 2 – 193, 3 – 213, 4 – 233, 5 – 253, 6 – 273, 7 – 293, 8 – 313, 9 – 333, 10 – 353, 11 – 373.

Fig. 3 *a*) presents the temperature dependence of the J_{SC} for the p-type c-Si HJT SCs under AM0 spectrum in the temperature range of 173–373 K. The experimental results demonstrate a linear increase in J_{SC} with rising temperature.

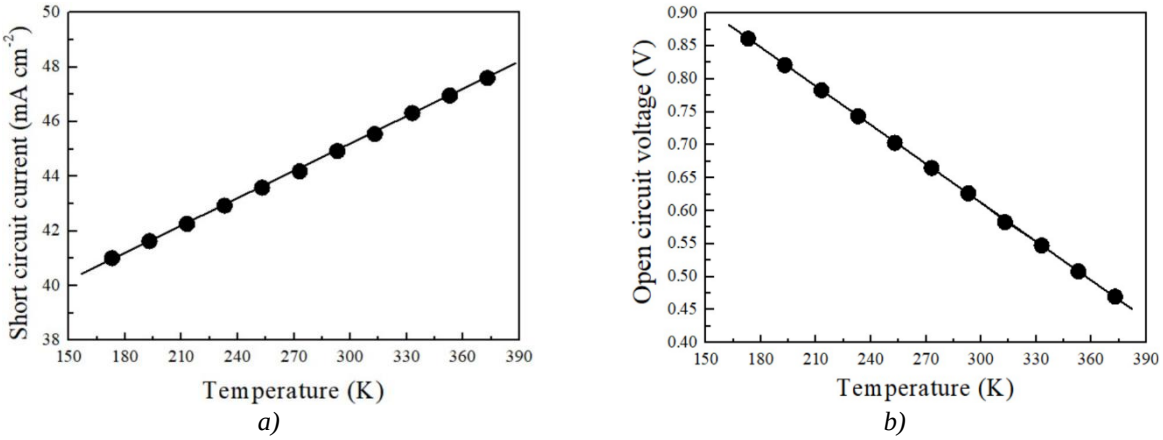

Fig. 3. Temperature dependence of short-circuit current density (*a*) and open-circuit voltage (*b*) of HJT SCs based on p-type c-Si wafer under AM0 spectrum (136.7 mW/cm^2).

For example, the J_{SC} value increased at a rate of approximately 0.032 mA/K, from 41.1 mA/cm² to about 47.5 mA/cm² in the range of 173 – 373 K. It is well known that the bandgap of c-Si narrows with increasing temperature [22], causing a redshift of the absorption edge toward longer wavelengths. Consequently, the wafer absorbs a broader range of the infrared spectrum, enhancing electron–hole pair generation in the photoactive region [16, 23]. Based on the experimental data, the temperature coefficient (TC) of the short-circuit current density (TCJ_{SC}) for the p-type c-Si HJT SCs was determined from the slope of the linear region of the $J_{SC}(T)$ dependence. The calculated TCJ_{SC} value was +(0.077±0.003) %/K, which is in good agreement with previously reported results [14-16]. Fig. 3 *b*) presents the experimental results of the temperature dependence of the open-circuit voltage - $V_{oc}(T)$, for the p-type c-Si HJT SCs under AM0 spectrum in the temperature range of 173–373 K. As shown in Fig. 3 *b*), the experimental value of the V_{oc} decreases linearly with increasing temperature. Specifically, V_{oc} decreases from 0.861 V at 173 K to 0.47 V at 373 K. The observed reduction in V_{oc} with increasing temperature is mainly caused by the temperature-dependent narrowing of the Si bandgap [22], which leads to an exponential increase in the reverse saturation current density (J_0) due to the higher intrinsic carrier concentration (n_i) [24].

According to our previous studies [25, 26], the temperature dependence of V_{oc} can be expressed as

$$V_{oc}(T) = \frac{E_g(T)}{q} - \frac{kT}{q}\ln\left\{\frac{N_{C0}N_{V0}}{\left[\frac{J_{SC}(T)}{q\left[\frac{D}{L_{diff}}tanh\left(\frac{d}{L_{diff}}\right)+S(T)\right]}\right]\left[N_a(T)+\frac{J_{SC}(T)}{q\left[\frac{D}{L_{diff}}tanh\left(\frac{d}{L_{diff}}\right)+S(T)\right]}\right]}\left(\frac{T}{T_0}\right)^3\right\} \quad (1)$$

where, D −ambipolar diffusion coefficient, d −base thickness, L_{diff} −minority carrier diffusion length, N_a −acceptor concentration, N_{C0} and N_{V0} − effective density of states in conduction and valence band at T_0=300 K, S −total surface recombination velocity ($S = S_0 + S_d$), S_0 and S_d −surface recombination velocity on the front and rear surfaces of wafer, respectively.

According to Equation (1), the parameters of the light J–V curves of the p-type c-Si HJT SCs, such as J_{SC}, total recombination velocity (S), including both surface ($S = S_0 + S_d$) and bulk $\tau(T)$ components at different temperatures, proposed in [27, 28], N_a and L_{diff} exhibit a tendency to increase with temperature. Within the investigated temperature range, the S in the p-type c-Si HJT SC increased from 12.8 cm/s at 173 K to 24.2 cm/s at 373 K, which is in good agreement with the data reported in [29]. The S, incorporating both surface ($S = S_0 + S_d$) and bulk $\tau(T)$ contributions at various temperatures, was evaluated using the approach proposed in [25-27]. The S noticeably increased from 9.65 cm/s to 18.6 cm/s after laser cutting at room temperature. The combined temperature-dependent variations of these parameters contribute to the observed decrease in V_{oc}.

The temperature coefficient of the open-circuit voltage (TCV_{oc}) for the p-type c-Si HJT SCs was determined from the slope of the linear region of the experimental $V_{oc}(T)$ dependence. The obtained value of TCV_{oc} was –(0.23±0.002)%/K in the temperature range of 173–373 K. Notably, this value is significantly lower than those reported for other c-Si-based PV technologies. It is also slightly smaller than the TCV_{oc} (–0.254%/K) obtained for n-type Si HJT SCs in [14-16], which can be attributed to the full rear-side silver (Ag) metallization in that structure. Such metallization hinders heat dissipation, thereby increasing the thermal sensitivity of the device. In addition, the TCV_{oc} of p-type c-Si HJT SCs also depends on the illumination level. According to [14-16], as the illumination intensity increases, the absolute value of TCV_{oc} decreases. Therefore, the relatively low TCV_{oc} observed in this study can be explained by measurements performed under the AM0 spectrum (136.7 mW/cm²). A smaller (less negative) TCV_{oc} reflects enhanced thermal stability, as the SC maintains a higher V_{oc} with increasing temperature.

Fig. 4 *a*) presents the experimental results of the temperature dependence of the fill factor - $FF(T)$, for the p-type c-Si HJT SCs under AM0 spectrum (136.7 mW/cm²). The FF is defined as follows [23]:

$$FF = \frac{J_m V_m}{J_{sc} V_{oc}}, \quad (2)$$

where, J_m and V_m are the current density and voltage at the maximum power point, respectively.

It can be seen from Fig. 4 *a*) the FF of the p-type c-Si HJT SCs decreases almost linearly from about 77.3% to 65.7% as the temperature increases from 173 K to 373 K. Within this temperature range, the series resistance (R_s) slightly decreases from about 3.43 Ω·cm^2 to 1.65 Ω·cm^2, as shown in Fig. 4 *b*). In the investigated temperature range, the shunt resistance (R_{sh}) exhibits only minor variations with temperature, as a results, a noticeable reduction in FF is observed at elevated temperatures.

The R_s of the p-type c-Si HJT SCs is determined from the linear region of the J-V curve near the V_{oc} point, while the R_{sh} is extracted from the linear region close to the J_{sc} point [30]. The total R_s comprises several resistive components connected in series with the p-n-junction, including the bulk resistances of the p- and n-type semiconductor regions, the metal–semiconductor contact resistances, and resistances of the front and rear metal contacts. The R_{sh} represents leakage current pathways through pinholes, surface recombination currents, tunneling via bulk defects, and peripheral leakage at the device edges [31].

It is well known that both the R_s and R_{sh} strongly influence the FF of SCs. To achieve a high FF, R_s must be minimized, while R_{sh} should be maximized [31]. In the present study, a clear decrease in R_s with increasing temperature was observed, which under typical conditions should result in an increase in FF. However, the experimental results revealed the opposite trend FF decreased with temperature. One of the main reasons for this discrepancy is the simultaneous slight reduction in R_{sh} due to parasitic leakage paths through the p-n-junction at elevated temperatures, and linear decrease in V_{oc} with temperature. According to Equation (2), FF is positively correlated with V_{oc}, therefore, the decrease in V_{oc} leads to a corresponding reduction in FF. As a result, the combined effect of decreasing R_{sh} and V_{oc} causes the deterioration of FF with increasing temperature, which is consistent with the experimental observations reported by other researchers [32].

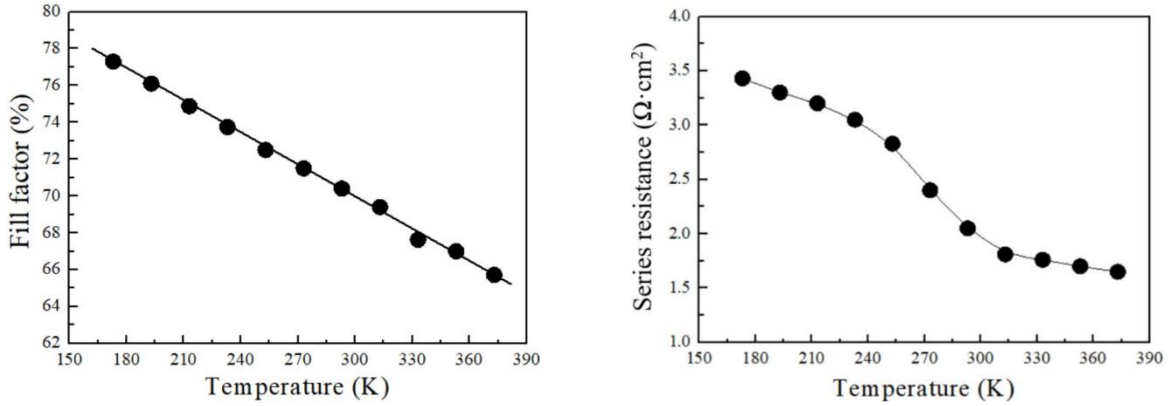

a) *b)*

Fig. 4. Temperature dependence of fill factor (*a*) and series resistance (*b*) of HJT SCs based on p-type c-Si wafer under AM0 spectrum (136.7 mW/cm^2).

The temperature coefficient of the fill factor ($TCFF$), determined from the slope of the linear region of the $FF(T)$ dependence, was found to be – (0.075±0.004) %/K in the temperature range of 173–373 K. To evaluate the contribution of V_{oc} and R_s to the $TCFF$ of p-type c-Si HJT SCs, the following expression was used, as described in [33].

$$\frac{1}{FF}\frac{dFF}{dT} = (1 - 1.02FF_0)\left(\frac{1}{V_{oc}}\frac{dV_{oc}}{dT} - \frac{1}{T}\right) - \frac{R_s}{\frac{V_{oc}}{I_{sc}} - R_s}\left(\frac{1}{R_s}\frac{dR_s}{dT}\right), \quad (3)$$

where,

$$FF_0 = \frac{\frac{qV_{oc}}{nkT} - ln\left(\frac{qV_{oc}}{nkT} + 0.72\right)}{\frac{qV_{oc}}{nkT} + 1}, \quad (4)$$

FF_0 is the FF in the absence of the R_s and R_{sh}, n −diode ideality factor, T − cell temperature, respectively.

From Eq. (3), it can be seen that the first term represents the contribution of the V_{oc} to the $TCFF$, while the second term reflects the contribution of the R_s to the $TCFF$. For the studied SCs, the analysis showed that the contribution of the V_{oc} to the $TCFF$ is dominant, accounting for more than 60%. Therefore, the observed

decrease in FF with increasing temperature can be explained by the strong temperature dependence of V_{oc}, which, as mentioned earlier, is primarily governed by the effective intrinsic carrier concentration ($n_{i.eff}$) that increases at elevated temperatures due to bandgap narrowing [22]. Fig. 5 shows the temperature dependence of the maximum power $P_{\max}(T)$ (*a*) and the conversion efficiency $\eta(T)$ (*b*) for the *p*-type c-Si HJT SCs under AM0 spectrum (136.7 mW/cm²). The $P_{\max}$ value is defined as the product of J_{sc}, V_{oc} and FF. As shown in Fig. 5 *a*)**,** the maximum power ($P_{\max}$) of the *p*-type c-Si HJT SCs decreases linearly from approximately 27.3 mW/cm² to 14.7 mW/cm² as the temperature increases from 173 K to 373 K. This behavior of $P_{\max}$ is primarily attributed to the temperature dependencies of key PV parameters such as J_{sc}, V_{oc}, FF and R_s, which collectively exert the most significant influence on the $P_{\max}(T)$ characteristics [34].

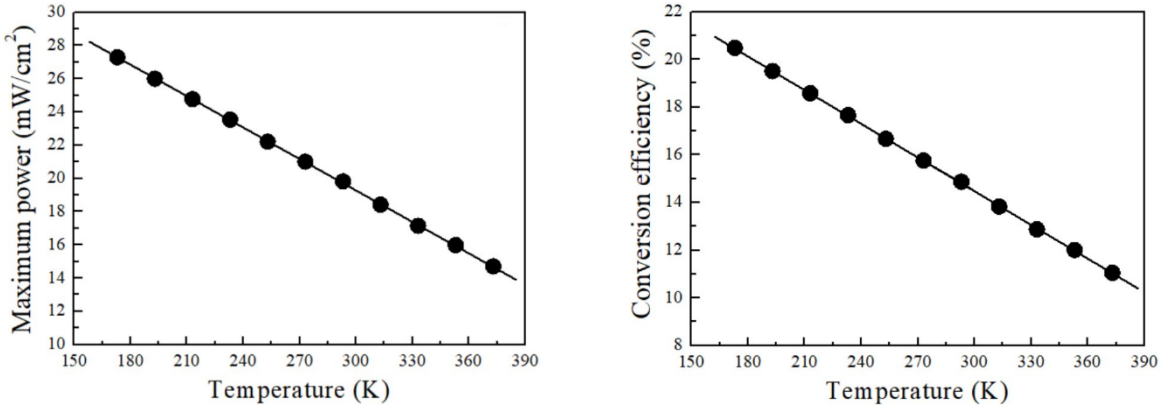

a) *b)*

Fig. 5. Temperature dependence of the maximum power (*a*) and conversion efficiency (*b*) of *p*-type c-Si HJT SCs under AM0 spectrum (136.7 mW/cm²) in the temperature range of 173–373 K.

The temperature coefficient of the P_{max} (TCP_{max}) was determined to be – (0.231±0.008) %/K in the investigated temperature range. The relatively low TCP_{max} of HJT SCs, compared with other Si-based PV technologies, can be attributed to the presence of intrinsic *a*-Si:H passivation layers on both surfaces of the c-Si wafer, which effectively suppress recombination losses of photogenerated charge carriers. This structural design leads to a reduction in the TCV_{oc}, which contributes more than 60% to the overall variation in the TCP_{max} and therefore plays a dominant role compared to other PV parameters such as J_{sc} and FF [15]. Owing to the excellent surface passivation provided by the intrinsic *a*-Si:H layers, low temperature HJT SCs currently achieve record-high V_{oc} (up to 752 mV) [12], which in turn accounts for their relatively low TCP_{max} values [14]. Fig. 5 *b*) presents the experimental results of the temperature dependence of the conversion efficiency, $\eta(T)$ of the *p*-type c-Si HJT SCs under AM0 spectrum (136.7 mW/cm²). The conversion efficiency η is defined as the ratio of the maximum power (P_{max}) to the incident light power (P_{rad}), which can be expressed by the following equation [31]:

$$\eta = \frac{P_{max}}{P_{rad}} \cdot 100\% = \frac{J_{sc}V_{oc}FF}{P_{rad}} \cdot 100\%, \quad (5)$$

where, P_{rad}= 136.7 mW/cm².

As shown in Fig. 5 *b*), the $\eta(T)$ of the *p*-type c-Si HJT SCs follows a trend similar to that of the P_{max}. As the temperature increased from 173 K to 373 K, the η value decreases linearly from 20.5% to 11.1%. The reduction in η with increasing temperature is primarily attributed to the temperature dependence of the key PV parameters of the SCs: V_{oc}, FF, and to a lesser extent, J_{sc}, since the η is defined by Eq. (5). It should also be noted that the η of the SCs under the AM0 spectrum is lower than under AM1.5G conditions. This difference primarily arises because the AM0 spectrum lacks atmospheric absorption, resulting in a higher proportion of ultraviolet (UV) and infrared (IR) radiation, which are less efficiently converted into electrical energy. This occurs because the spectral response, or internal quantum efficiency (IQE) of SCs is significantly lower in these regions of the solar spectrum [35]. After laser cutting, the η of the *p*-type HJT SCs was determined to be 14.9% under AM0 and 16.3% under AM1.5G spectrum at room temperature.

4. Conclusion

In this study, the light J-V curves of HJT SCs fabricated on boron-doped p-type c-Si wafers were experimentally investigated under extraterrestrial AM0 spectrum (136.7 mW/cm²) over the temperature range of 173–373 K. The experimental results revealed a linear increase in the J_{sc} with rising temperature, whereas the V_{oc}, FF and P_{max} exhibited a linear decrease.

The TCs of the key PV parameters were determined as follows: the J_{sc} exhibited a positive temperature coefficient of +(0.077±0.003) %/K, while the V_{oc} and FF showed negative coefficients of –(0.23±0.002)%/K and –(0.075±0.004)%/K, respectively, within the investigated temperature range. The maximum power reached 27.3 mW/cm² at 173 K, with a corresponding power temperature coefficient (TCP_{max}) of –(0.231±0.008)%/K - one of the lowest values reported for Si-based PV technologies. This remarkably low temperature coefficient demonstrates the excellent thermal stability of p-type c-Si HJT SCs, primarily attributed to the effective surface passivation provided by the intrinsic a-Si:H layers on both wafer surfaces.

It is well established that n-type Si-based SCs are predominantly used in terrestrial PV applications due to their high conversion efficiency and superior surface passivation quality. However, for space applications, transitioning to p-type Si wafers offer distinct advantages, as they exhibit greater radiation tolerance, reduced susceptibility to radiation-induced degradation, and a lower TCP_{max}. These characteristics are critical for ensuring long-term operational stability and reliability in harsh extraterrestrial environments. Consequently, p-type c-Si HJT SCs represent highly promising candidates for power generation in small satellite platforms (CubeSats) and other spacecraft operating in LEO, where wide temperature fluctuations and stringent energy efficiency requirements make thermal robustness a key design consideration.

Conflict of interest statement

The authors declare that they have no conflict of interest in relation to this research, whether financial, personal, authorship or otherwise, that could affect the research and its results presented in this paper.

CRediT author statement

Utamuradova Sh.B.: Conceptualization, Writing – original draft; **Terukov E.I.:** Resources, Supervision, Writing – review & editing; **Ataboev O.K., Kabulov R.R.:** Investigation, Writing – original draft; **Panaiotti I.E.:** Formal analysis, Writing – review & editing; **Uzakbayeva N.S.:** Investigation, Methodology.

The final manuscript was read and approved by all authors.

Acknowledgements

The authors are grateful to the staff of the R&D Center for Thin Film Technologies in Energetics, Ioffe Institute, and Zh.I. Alferov St. Petersburg National Research Academic University for valuable assistance in the process of creating and studying HJT SCs, as well as to the staff of the Semiconductor Physics and Microelectronics research institute for valuable advice when discussing the research results.

References

1 Aljohani A.J., Mirza J., Ghafoor S.A. (2021) A novel regeneration technique for free space optical communication systems. *IEEE Communications Letters*, 25(1), 196–199. https://doi.org/10.1109/LCOMM.2020.3029591

2 Kalinovskii V.S., Terukov E.I., Abolmasov S.N., Prudchenko K.K., Kontrosh E.V., Tolkachev I.A., Kochergin A.V., Titov A.S., Ataboev O.K. (2023) Studies of degradation silicon heterojunction solar cells by 1 MeV electrons irradiation. *Applied Solar Energy*, 59(5), 604–611. https://doi.org/10.3103/S0003701X23600984

3 Utamuradova Sh.B., Terukov E.I., Ataboev O.K., Panaiotti I.E., Kabulov R.R., Troshin A.V. (2025) Influence of 1 MeV electron irradiation on the output parameters of silicon heterojunction solar cells. *Nuclear Instruments and methods in physics research section B: Beam interactions with materials and atoms*, 560, 165630. https://doi.org/10.1016/j.nimb.2025.165630

4 Verduci R., Romano V., Brunetti G., Nia N.Y., Carlo A.D., D'Angelo G., Ciminelli C. (2022) Solar energy in space applications: review and technology. *Advanced Energy Materials*, 12(29), 2200125. https://doi.org/10.1002/aenm.202200125

5 Li J., Aierken A., Liu Y., Zhuang Y., Yang X., Mo J.H., Fan R.K., Chen Q.Y., Zhang S.Y., Huang Y.M., Zhang Q. (2021) A brief review of high efficiency III-V solar cells for space application. *Frontiers in Physics*, 8, 631925. https://doi.org/10.3389/fphy.2020.631925

6 Yamaguchi M., Takamoto T., Araki K., Ekins-Daukes N. (2005) Multi-junction III-V solar cells: Current status and future potential. *Solar Energy*, 79(1), 78–85. https://doi.org/10.1016/j.solener.2004.09.0186

7 Suzuki A., Kaneiwa M., Saga T., Matsuda S. (1999) Progress and future view of silicon space solar cells in Japan. *IEEE Transactions on Electron Devices*, 46(10), 2126–2132. https://doi.org/10.1109/16.792007

8 Rehman, A.U., Lee, S.H. & Lee, S.H. (2016) Silicon space solar cells: progression and radiation-resistance analysis. *Journal of the Korean Physical Society,* 68, 593–598. https://doi.org/10.3938/jkps.68.593

9 Kaltenbrunner M., Adam G., Glowacki E.D., Drack M., Schwödiauer R., Leonat L., Apaydin D.H., Groiss H., Scharber M.C., White M.S., Sariciftci N.S., Bauer S. (2015) Flexible high power-per-weight perovskite solar cells with chromium oxide-metal contacts for improved stability in air. *Nature Materials*, 14, 1032-1039. https://doi.org/10.1038/nmat4388

10 Fernandez J., Janz S., Suwito D., Oliva E., Dimroht F. (2008) Advanced concepts for high- efficiency germanium photovoltaic cells. *Proceeding of the 33rd IEEE Photovoltaic Specialists Conference*, San Diego, CA, USA. https://doi.org/10.1109/PVSC.2008.4922631

11 Nishioka K., Takamoto T., Agui T., Kaneiwa M., Uraoka Y., Fuyuki T. (2006) Evaluation of InGaP/InGaAs/Ge triple-junction solar cell and optimization of solar cell's structure focusing on series resistance for high-efficiency concentrator photovoltaic systems. *Solar Energy Materials and Solar Cells*, 90(9), 1308–1321, https://doi.org/10.1016/j.solmat.2005.08.003

12 Green M.A., Dunlop E.D., Yoshita M., Kopidakis N., Bothe K., Siefer G., Hao X., Jiang J.Y. (2025) Solar cell efficiency tables (Version 66). *Progress in Photovoltaics: Research and applications*, 33(7), 795–810. https://doi.org/10.1002/pip.3919

13 Joseph K.L.V., Rosana N.T.M., Kumar J.A., Samrot A.V. (2025) Commercial bifacial silicon solar cells – Characteristics, module topology and passivation technique for high electrical output: An overview. *Results in Engineering*, 26, 104971. https://doi.org/10.1016/j.rineng.2025.104971

14 Le A.H.T., Dreon J., Michel J.I., Boccard M., Bullock J., Borojevic N., Hameiri Z. (2022) Temperature-dependent performance of silicon heterojunction solar cells with transition-metal-oxide-based selective contacts. *Progress in Photovoltaics: Research and applications*, 30, 981–993. https://doi.org/10.1002/pip.3509

15 Le A.H.T., Basnet R., Yan D., Chen W., Nandakumar N., Duttagupta Sh., Seif J.P., Hameiri Z. (2021) Temperature-dependence performance of silicon solar cells with polysilicon passivating contacts. *Solar Energy Materials and Solar Cells*, 225, 111020. https://doi.org/10.1016/j.solmat.2021.111020

16 Haschke J., Seif J.P., Riesen Y., Tomasi A., Cattin J., Tous L., Choulat P., Aleman M., Cornagliotti E., Uruena A., Russell R., Duerinckx F., Champliaud J., Levrat J., Abdallah A.A., Aissa B., Tabet N., Wyrsch N., Despeisse M., Szlufcik J., Wolf S.D., Ballif C. (2017) The impact of silicon solar cell architecture and cell interconnection on energy yield in hot and sunny climates. *Energy and environmental science*, 10(5), 1–11. https://doi.org/10.1039/C7EE00286F

17 Cardinaletti I., Vangerven T., Nagels S., Cornelissen R., Schreurs D., Hruby J., Vodnik J., Devisscher D., Kesters J., D'Haen J., Franquet A., Spampinato V., Conard T., Maes W., Deferme W., Manca J.V. (2018) Organic and perovskite solar cells for space application. *Solar Energy Materials and Solar Cells*, 182, 121-127. https://doi.org/10.1016/j.solmat.2018.03.024

18. Ataboev O.K., Terukov E.I., Shelopin G.G., Kabulov R.R. (2021) Wet chemical treatment of monocrystalline silicon wafer surfaces. *Applied Solar Energy*, 57(5), 363–369. https://doi.org/10.3103/S0003701X21050042

19 Hammann B., Schindler F., Schön J., Kwapil W., Schubert M.C., Glunz S.W. (2025) Review on hydrogen in silicon solar cells: From its origin to its detrimental effects. *Solar Energy Materials and Solar Cells*, 282, 113432. https://doi.org/10.1016/j.solmat.2025.113432

20 Han H., Jia X., Ma C., Wu Y. (2022) A novel laser scribing method combined with the thermal stress cleaving for the crystalline silicon solar cell separation in mass production. *Solar Energy Materials and Solar Cells*, 240, 111714. https://doi.org/10.1016/j.solmat.2022.111714

21 Witteck R., Hinken D., Schulte-Huxel H., Vogt M.R., Müller J., Blankemeyer S., Köntges M., Bothe K., Brendel R. (2016) Optimized interconnection of passivated emitter and rear cells by experimentally verified modeling. *IEEE Journal of Photovoltaics*, 6(2), 432-439. https://doi.org/10.1109/JPHOTOV.2016.2514706

22 Bludau W., Onton A., Heinke W. (1974) Temperature dependence of the band gap of silicon. *Journal of Applied Physics*, 45(4), 1846–1848. https://doi.org/10.1063/1.1663501

23 Ataboev O.K., Kabulov R.R., Matchanov N.A., Egamov S.R. (2019) Influence of temperature on the output parameters of a photovoltaic module based on amorphous hydrogenated silicon. *Applied solar energy*, 55(3), 159–167. https://doi.org/10.3103/S0003701X19030022

24 Löper P., Pysch D., Richter A., Hermle M., Janz S., Zacharias M., Glunz S.W. (2012) Analysis of the temperature dependence of the open-circuit voltage. *Energy Procedia*, 27, 135-142. https://doi.org/10.1016/j.egypro.2012.07.041

25 Utamuradova Sh.B., Terukov E.I., Ataboev O.K., Panaiotti I.E., Baranov A.I., Mikhaylov O.P. (2025) A study on the influence of temperature on the output parameters of silicon heterojunction solar cells. *Journal of computational electronics*, 24, 162. https://doi.org/10.1007/s10825-025-02400

26 Ataboev O.K., Utamuradova Sh.B., Panaiotti I.E., Terukov E.I., Malevskiy D.A., Baranov A.I., Troshin A.V. (2026) Temperature dependence of photovoltaic performance of silicon heterojunction solar cells based on gallium- and

phosphorous-doped silicon wafers. *Radiation Physics and Chemistry*, 240, 113407. https://doi.org/10.1016/j.radphyschem.2025.113407

27 Panaiotti I.E., Terukov E.I. (2019) A study of the effect of radiation on recombination loss in heterojunction solar cells based on single-crystal silicon. *Technical physics letters*, 45(3),193–196. https://doi.org/10.1134/S106378501903012X

28 Panaiotti I.E., Terukov E.I., Shakhrai I.S. (2020) A method for calculating operating characteristics of silicon heterojunction solar cells with arbitrary parameters of crystalline wafers. *Technical physics letters*, 46, 835–837. https://doi.org/10.1134/S1063785020090072

29 Bernardini S., Bertoni M.I. (2019) Insights into the degradation of amorphous silicon passivation layer for heterojunction solar cells. *Physica status solidi (a)*, 216(4), 1800705. https://doi.org/10.1002/pssa.201800705

30 Singh P., Ravindra N.M. (2012) Analysis of series and shunt resistance in silicon solar cells using single and double exponential models. *Emerging materials research*, 1(1), 33 – 38. https://doi.org/10.1680/emr.11.00008

31 Fahrenbruch A.L., Bube R.H., (1983). *Fundamentals of solar cells. Photovoltaic solar energy conversion*. London. https://doi.org/10.1016/B978-0-12-247680-8.X5001-4

32 Büyükbaş-Uluşan A., Turan R., Altındal Ş. (2025) On the investigation of current transport mechanisms (CTMs) of the crystalline Si solar cells utilizing current/voltage (I-V) characteristics in temperature range of 110-380 K. *Journal of materials science: Materials in electronics*, 36, 1173. https://doi.org/10.1007/s10854-025-15235-7

33 Durpe O., Vaillon R., Green M.A. (2015) Physics of the temperature coefficients of solar cells. *Solar Energy Materials and Solar Cells*, 140, 92-100. https://doi.org/10.1016/j.solmat.2015.03.025

34 Green M.A. (2003). General temperature dependence of solar cell performance and implications for device modelling. *Progress in Photovoltaics: Research and Applications*, 11(5), 333-340. https://doi.org/10.1002/pip.496

35 Woodyard J.R., Landis G.A. (1991) Radiation resistance of thin-film solar cells for space photovoltaic power. *Solar cells*, 31(4), 297. https://doi.org/10.1016/0379-6787(91)90103-V

AUTHORS' INFORMATION:

Utamuradova, Sharifa Bekmuradovna – DSc, Professor, Semiconductor Physics and Microelectronics research institute, Tashkent, Uzbekistan; Scopus Author ID: 6506286512; https://orcid.org/0000-0002-1718-1122; sh-utamuradova@yandex.com

Terukov, Evgeniy Ivanovich – DSc, Professor, Ioffe Institute, Russian Academy of Sciences, St. Petersburg, Russia; Scopus Author ID: 9236174500; https://orcid.org/0000-0002-5226-1101; eug.terukov@mail.ioffe.ru

Ataboev, Omonboy Kurbanboevich – PhD, Senior researcher, Semiconductor Physics and Microelectronics research institute, Tashkent, Uzbekistan; Scopus Author ID: 54890775800; https://orcid.org/0000-0002-5226-1101; omonboy12@mail.ru

Kabulov, Rustam Rashidovich – PhD, Senior researcher, Physical-technical Institute Uzbekistan Academy of Sciences, Tashkent, Uzbekistan; Scopus Author ID: 6602800668; https://orcid.org/0000-0003-3157-9038; krr1982@bk.ru

Panaiotti, Irina Evgenevna – PhD, Senior researcher, Ioffe Institute, Russian Academy of Sciences, St. Petersburg, Russia; Scopus Author ID: 6504074762; https://orcid.org/0000-0003-1233-7973; panaiotti@mail.ioffe.ru

Uzakbayeva, Nargiza Sansizbayevna – Master, Senior Lecturer, Nukus state technical university, Nukus, Uzbekistan; https://orcid.org/0009-0008-3900-2421; nargizauzakbaeva4@gmail.com